Organostannoxane-Supported Multiferrocenyl Assemblies: Synthesis, Novel Supramolecular Structures, and Electrochemistry

Vadapalli Chandrasekhar,*[a] Kandasamy Gopal,[a] Selvarajan Nagendran,[a] Puja Singh,[a] Alexander Steiner,[b] Stefano Zacchini,[b] and Jamie F. Bickley[b]

Abstract: Organostannoxane-based multiredox assemblies containing ferrocenyl peripheries have been readily synthesized by a simple *one-pot* synthesis, either by a solution method or by room-temperature solid-state synthesis, in nearly quantitative yields. The number of ferrocenyl units in the multiredox assembly is readily varied by stoichiometric control as well as by the choice of the organotin precursors. Thus, the reaction of the diorganotin oxides, R_2SnO (R = Ph, *n*Bu and *t*Bu) with ferrocene carboxylic acid affords tetra-, di-, and mononuclear derivatives $[\{Ph_2Sn[OC(O)Fc]_2\}_2]$ (**1**), $[\{[nBu_2SnOC(O)Fc]_2O\}_2]$ (**2**), $[nBu_2Sn\{OC(O)Fc\}_2]$ (**3**), $[\{tBu_2Sn(OH)OC(O)Fc\}_2]$ (**4**), and $[tBu_2Sn\{OC(O)Fc\}_2]$ (**5**) (Fc = $\eta^5C_5H_4$-Fe-$\eta^5C_5H_5$). The reaction of triorganotin oxides, $R_3SnOSnR_3$ (R = *n*Bu and Ph) with ferrocene carboxylic acid leads to the formation of the mono-nuclear derivatives $[Ph_3SnOC(O)Fc]$ (**6**) and $[\{nBu_3SnOC(O)Fc\}_n]$ (**7**). Molecular structures of the compounds **1–4** and **6** have been determined by single-crystal X-ray analysis. The molecular structure of compound **1** is new among organotin carboxylates. In this compound, ferrocenyl carboxylates are involved in both chelating and bridging coordination modes to the tin atoms to form an eight-membered cyclic structure. In all of these compounds, the acidic protons of the cyclopentadienyl groups are hydrogen bonded to the carboxylate oxygens (C–H···O) to form rich supramolecular assemblies. In addition to this, π–π, T-shaped, L-shaped, and side-to-face stacking interactions involving ferrocenyl groups also occur. Compound **6** shows an interesting and novel intermolecular CO_2–π stacking interaction. Electrochemical analysis of the compounds **1–4**, **6**, and **7** shows a single, quasi-reversible oxidation peak corresponding to the simultaneous oxidation of four, two, and one ferrocenyl substituents, respectively. Compound **5** shows two quasi-reversible oxidation peaks. This is attributed to the positional difference among the ferrocenyl substituents on the tin atom. Additionally, while compounds **2** and **4** are electrochemically quite robust and do not decompose even after ten continuous CV cycles, compounds **1**, and **3**, **5–7** start to show decomposition after five cycles.

Keywords: electrochemistry · ferrocenyl derivatives · hydrogen bonds · organotin compounds · supramolecular chemistry

Introduction

Multimetallocenyl assemblies in general, and multiferrocenyl compounds in particular, have been attracting considerable interest in view of their potential applications as multielectron reservoirs, electron-transfer mediators, electrode-modification materials, ion sensors, or as materials for electronic devices.[1] We have been interested in the design of ferrocenyl assemblies containing multiple but electrochemically equivalent ferrocene units. In the literature, most of the strategies for the preparation of such compounds are based on a divergent approach and start (usually) from a central organic core which supports a periphery of electroactive ferrocene subunits.[2,3] In a completely different approach we have demonstrated that the use of inorganic frameworks, such as stannoxanes or cyclophosphazenes, as supports can lead to a one-step synthesis of hexaferrocenyl derivatives.[4] Subsequently, there have also been other reports on the use of supports derived from inorganic rings or cages.[5]

The advantages of using stannoxane frameworks for the construction of multiferrocenyl assemblies are manifold.

[a] Prof. Dr. V. Chandrasekhar, K. Gopal, S. Nagendran, P. Singh
Department of Chemistry
Indian Institute of Technology, Kanpur-208 016 (India)
Fax: (+91) 512-597-259
E-mail: vc@iitk.ac.in

[b] Dr. A. Steiner, S. Zacchini, J. F. Bickley
Department of Chemistry
University of Liverpool, Liverpool L69 7ZD (UK)

Supporting information for this article is available on the WWW under http://www.chemeurj.org/ or from the author.

 DOI: 10.1002/chem.200500316

Firstly, the stannoxane frameworks are reasonably robust. Secondly and importantly, the stannoxane cores are themselves not redox active.[1e,4a,4b] Thus, the support does not interfere with the electrochemical properties of the peripheral redox-active ferrocene units. Thirdly, the utilization of stannoxanes as supports allows a ready modulation of the *number* and *orientation* of the ferrocene units. Lastly, the favorable disposition of the oxygen centers and the aromatic hydrogen atoms allows the formation of interesting supramolecular structures in the solid state.[4b] In order to test the efficacy of these principles we have investigated the reactions of $(Ph_2SnO)_n$, $(nBu_2SnO)_n$, $(tBu_2SnO)_3$, $(Ph_3Sn)_2O$, and $(nBu_3Sn)_2O$ with ferrocene carboxylic acid. Herein, we describe the synthesis and electrochemical studies of $[\{Ph_2Sn[OC(O)Fc]_2\}_2]$ (**1**), $[\{[nBu_2SnOC(O)Fc]_2O\}_2]$ (**2**), $[nBu_2Sn\{OC(O)Fc\}_2]$ (**3**), $[\{tBu_2Sn(OH)OC(O)Fc\}_2]$ (**4**), $[tBu_2Sn\{OC(O)Fc\}_2]$ (**5**), $[Ph_3SnOC(O)Fc]$ (**6**), and $[\{nBu_3SnOC(O)Fc\}_n]$ (**7**) ($Fc = \eta^5C_5H_4\text{-Fe-}\eta^5C_5H_5$). The X-ray crystal structures of **1**–**4** and **6** are also described. The structure of **1** represents a new structural form of organotin carboxylates and reveals the formation of an eight-membered $Sn_2C_2O_4$ ring containing two bridging carboxylates. Although the structure of **2** was reported earlier[6] (as a benzene solvate), we have reinvestigated its nonsolvated form with the view of elucidating the supramolecular interactions that are present. All of these compounds (**1**–**4** and **6**) show an intricate supramolecular organization in the solid state that results from a cumulative effect of intermolecular secondary interactions. Aromatic interactions (π–π) among aryl rings have been well documented.[7] In contrast, such studies on ferrocenyl derivatives are limited.[8] The present work demonstrates the wide range of interferrocenyl interactions that are possible in the solid state and testifies to the efficacy of the growing field of organometallic crystal engineering. We also discuss the presence of a new CO_2–π supramolecular synthon in the crystal structure of **6**. The crucial role of the Sn_2O_2 distannoxane core vis-à-vis simple Sn–O linkages in terms of providing an ideal structural platform for generating a robust and stable electrochemical behavior for the multiferrocene assemblies has also been delineated.

Results and Discussion

The advantages of utilizing organostannoxanes as supports for constructing multiferrocene architectures are as follows. The number of ferrocene units in the eventual molecular assembly can be readily tuned by varying the nature of the organotin precursor. Additionally, unlike in the ferrocene assemblies synthesized by using organic supports, a common synthetic strategy is applicable in the present study. In all cases, the ferrocenyl assemblies were isolated in excellent yields (see Experimental Section). As we will also show below, the stannoxane frameworks are electrochemically inert and do not interfere with the electrochemical properties of the peripheral ferrocenes.

Synthetic aspects: All the organotin oxides reacted with ferrocene carboxylic acid to afford various types of products. The nature of the product depends upon the type of the organotin oxide as well as the stoichiometry of the reaction.[9] In addition, all the reactions can be carried out by the *traditional* synthetic route, namely, in a solvent such as toluene under reflux conditions and by using a Dean–Stark apparatus, which assists in the dynamic removal of water.[4a,b] Alternatively, a novel *solvent-free* methodology, which we have recently demonstrated, can also be adopted.[10] In this latter technique the reactants are ground together for a specified period of time. This was followed by a workup to afford the final products (see Experimental Section). Notably, the solvent-free synthesis also afforded the same products (in nearly the same yields) as those obtained by the traditional synthesis route.

The reaction of ferrocene carboxylic acid with $(Ph_2SnO)_n$ in a 1:1 or 2:1 stoichiometric ratio afforded exclusively the dinuclear compound $[\{Ph_2Sn[OC(O)Fc]_2\}_2]$ (**1**) (Scheme 1).

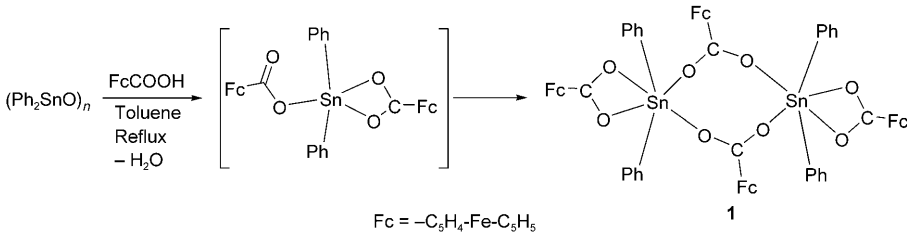

Scheme 1. Synthesis of compound **1**.

The poor solubility of **1** in many organic solvents prevented its molecular-weight measurement in solution. However, we were able to obtain a ^{119}Sn NMR spectrum in $CDCl_3$. A single resonance at $\delta = -321.4$ ppm was observed. This chemical shift is consistent with the coordination environment around tin[9] (2 C, 4 O) as well its cyclic structure (vide infra). The reaction of $(nBu_2SnO)_n$ with ferrocene carboxylic acid in toluene in a 1:1 ratio yielded the tetranuclear tin derivative $[\{[nBu_2SnOC(O)Fc]_2O\}_2]$ (**2**) (Scheme 2). In contrast, the reaction of $(tBu_2SnO)_3$ with ferrocene carboxylic acid under analogous reaction conditions afforded a hydroxy-bridged dimer, $[\{tBu_2Sn(OH)OC(O)Fc\}_2]$ (**4**) (Scheme 3). If the reactions were carried out using a 1:2 stoichiometry (R_2SnO:FcCOOH) mononuclear tin derivatives $[nBu_2Sn\{OC(O)Fc\}_2]$ (**3**) (Scheme 2) and $[tBu_2Sn\{OC(O)Fc\}_2]$ (**5**) (Scheme 3) were obtained. The reactions of the triorganotin derivatives $(R_3Sn)_2O$ with two equivalents of ferrocene carboxylic acid resulted in $[Ph_3SnOC(O)Fc]$ (**6**)

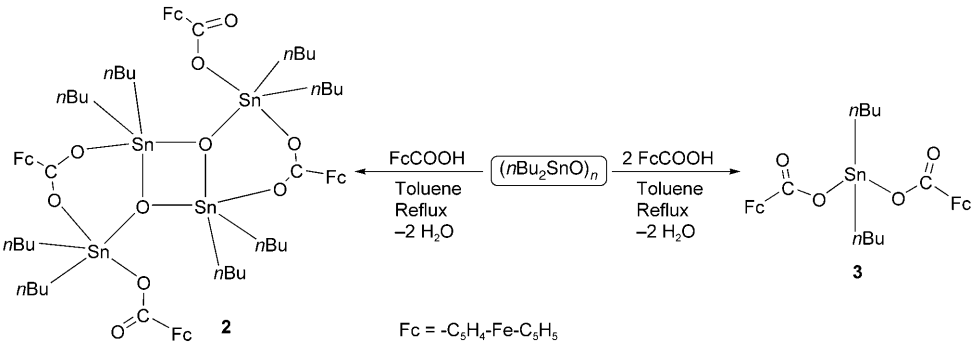

Scheme 2. Synthesis of compounds **2** and **3**.

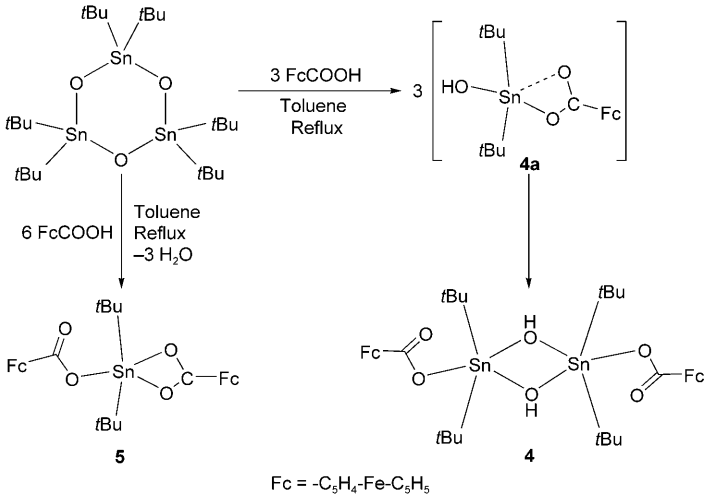

Scheme 3. Synthesis of compounds **4** and **5**.

or [{nBu$_3$SnOC(O)Fc}$_n$] (**7**) (Scheme 4). The ^{119}Sn chemical shifts of compounds **2**–**7** are given in the Experimental Section and are consistent with their molecular structures (vide infra).[9]

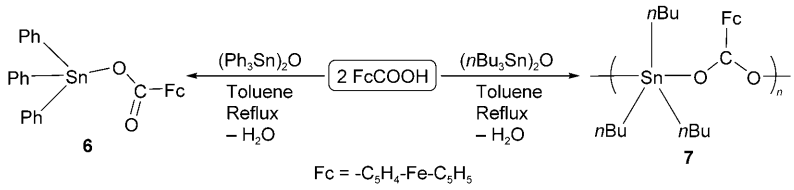

Scheme 4. Synthesis of compounds **6** and **7**.

X-ray crystal structures of compounds 1–4 and 6: The molecular structures of **1**–**4** and **6** are shown in Figure 1 and some of their selected metric parameters are summarized in Table 1.

The dinuclear derivative [{Ph$_2$Sn[OC(O)Fc]$_2$}$_2$] (**1**) is a new structural form of a diorganotin dicarboxylate, [R$_2$Sn(O$_2$CR′)$_2$]. In general diorganotin dicarboxylates are mononuclear complexes,[9] in which the tin is six-coordinate arising from an anisobidentate chelating coordination mode of the two carboxylates. As an example, the structure of compound **3** will be discussed below. The molecular structure of **1** contains two diphenyltin units and four ferrocene carboxylates (Figure 1). The two tin atoms present in the molecule are bridged by two ferrocene carboxylates in an anisobidentate coordination mode. This results in the formation of an eight-membered ring (Sn1, O3, C24, O4, Sn1*, O3*, C24*, and O4*). Each of the other two ferrocene carboxylates binds exclusively to one tin atom in an anisobidentate chelating coordination mode. The eight-membered Sn$_2$O$_4$C$_2$ ring is nearly planar with an average deviation of 0.024 Å from the mean plane. The planes of the terminal chelating carboxylates are also coplanar with the plane of the central Sn$_2$O$_4$C$_2$ cyclic core with a deviation angle of 3.15°. In compound **1**, two ferrocenyl moieties lie above and the other two lie below the plane of the Sn$_2$C$_2$O$_4$ core. An interesting aspect of the molecular organization of **1** is that the phenyl substituents present on one tin atom (Sn1) are found in an eclipsed conformation to those on the other tin atom (Sn1*). The intercentroid distance between the two phenyl groups is 3.735(5) Å. Each tin atom in compound **1** is six-coordinate with a distorted octahedral geometry. The axial positions are occupied by two phenyl substituents (C1 and C7) and the equatorial positions by four carboxylate oxygen atoms (O1, O2, O3, and O4*). Along the octahedral edge an additional weaker bonding interaction was found between tin and the bridging carboxylate oxygen atom (Sn1–O4 2.613(7) Å). Considering this interaction, the coordination number of the tin atom increases to seven and the geometry may be described as a distorted pentagonal bipyramid. Although cyclic rings of tin with carboxylate ligands are rare,[11] there have been recent reports on tin-containing inorganic rings with phosphinate and sulfonate ligands.[12]

The molecular structure of **2** shows that the four ferrocene moieties present in this compound are supported by a planar Sn$_4$O$_2$ core. This contrasts with the situation found in

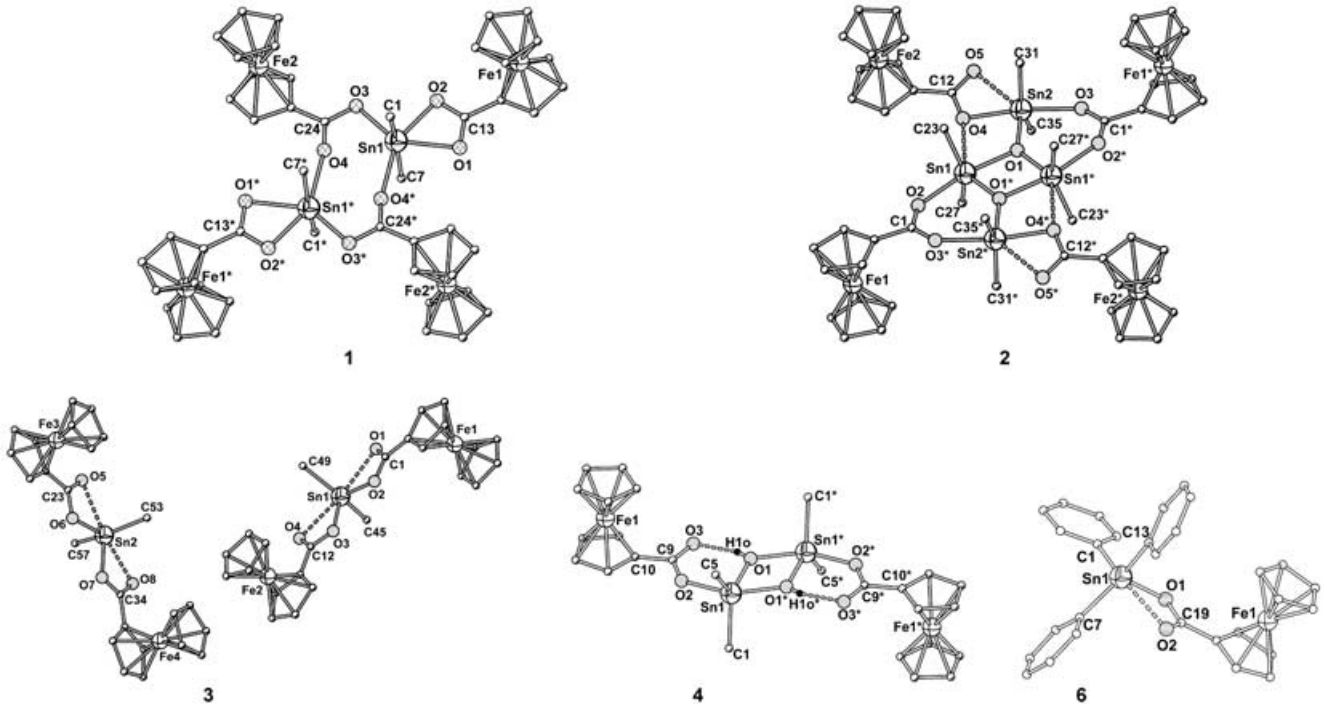

Figure 1. Molecular structures of compounds **1**–**4** and **6**.

[{*n*BuSn(O)OC(O)Fc}$_6$], in which the six ferrocene units are located in a wheel-like arrangement around a central Sn_6O_6 prismane core.[4a] Compound **2** adopts the familiar ladder framework and has two central and two terminal tin atoms. The ferrocene carboxylates are involved in both anisobidentate chelating (Sn2–O4 2.201(18) and Sn2–O5 2.646(18) Å) as well as isobidentate bridging (Sn1*–O2* 2.243(19) and Sn2–O3 2.249(19) Å) coordination modes. The Sn–O distances in the central Sn_2O_2 unit of **2** are as follows: Sn1–O1 2.168(18) and Sn1–O1* 2.036(17) Å (cf. metric parameters for analogous Sn–O bonds in [{*n*BuSn(O)OC(O)Fc}$_6$][4a] are: Sn1–O3 2.106(4), Sn1–O1 2.100(4), Sn2–O3 2.087(3), and Sn2–O1 2.099(4) Å).

The mononuclear tin dicarboxylate **3** crystallizes as a hexane solvate. The unit cell contains two independent molecules in the asymmetric unit. They are perpendicular to each other and are interact through L-shaped stacking of the ferrocenyl moieties (as discussed vide infra). The two ferrocenyl moieties are attached to the tin atom through the chelating carboxylate ligands (anisobidentate coordination mode). The tin atom is six-coordinate with a 2C, 4O coordination environment. The geometry around the tin atom can be described as a skewed trapezoidal bipyramid.[13] The orientations of the ferrocenyl units in the two independent molecules present in the asymmetric unit are different. While in one molecule the two ferrocenes are on the same side of the plane containing the tin and the carboxylate oxygen atoms, in the second molecule the two ferrocene moieties are *trans* to each other.

Interestingly, while the 1:1 reaction of $(n\mathrm{Bu_2SnO})_n$ with FcCOOH afforded the tetranuclear derivative [{[nBu$_2$SnOC(O)Fc]$_2$O}$_2$] (**2**), the analogous reaction involving $(t\mathrm{Bu_2SnO})_3$ afforded the dinuclear derivative [{tBu$_2$Sn(OH)OC(O)Fc}$_2$] (**4**). The steric bulk of the *tert*-butyl substituents clearly plays an important role in this reaction and limits the nuclearity of the tin assembly. Puff and co-workers have previously shown that [tBu$_2$Sn(OH)(X)]$_2$ (X = F, Cl, OH) is dimeric.[14] It is reasonable to propose that the dinuclear structure of **4** arises from a dimerization of the mononuclear monohydroxy derivative **4a** (Scheme 3). Such dimerization of intermediates to eventual products has been reported by our group recently.[15] The two tin atoms in **4** are bridged by two hydroxyl groups (O1 and O1*) to generate a central Sn_2O_2 stannoxane core. Each tin atom is bound to one ferrocene carboxylate and only one oxygen atom (O2) of the ferrocene carboxylate is bound to the tin atom. The other oxygen atom of the carboxylate (O3) is involved in an intramolecular hydrogen bonding with the bridging OH group. Thus, each tin atom in **4** is five-coordinate (2C, 3O coordination environment) and has a distorted trigonal bipyramidal geometry. Two *tert*-butyl groups (C1 and C5) and one bridging hydroxyl oxygen atom (O1) occupy equatorial positions, while one carboxylate oxygen atom (O2) and the other bridging hydroxyl oxygen atom (O1*) are the axial ligands. The average Sn–O bond length for the planar distannoxane core is 2.106(2) Å, which is comparable with that found in [{tBu$_2$Sn(OH)OC(O)CH$_3$}$_2$] (2.125 Å)[16] as well as in **2**.

The molecular structure of **6** shows that the triorganotin carboxylate adopts a discrete structure that is in accordance with the preference of such structures for triphenyltin arylcarboxylates.[9,10] The tin atom is involved in four covalent

Table 1. Structural description of compounds **1–4** and **6** along with their bonding parameters.

Compounds/ structural forms	Coordination mode of carboxylate and environment around tin	Sn–O [Å][a] (carboxylate)	Sn–O [Å][a] (core)	Angles [°][a]
[{$Ph_2Sn[OC(O)Fc]_2$}$_2$] (**1**) carboxylate-bridged dinuclear tetracarboxylate	anisobidentate bridging and chelating six-coordinate (2C, 4O) distorted octahedral geometry	Sn1–O1 2.333(3) Sn1–O2 2.163(3) Sn1–O3 2.162(3) Sn1–O4* 2.486(3) Sn1–O4 2.613(4)		C1-Sn1-C7 165.04(17) O1-Sn1-O3 143.06(11) O1-Sn1-O4* 91.89(10) O2-Sn1-O3 84.91(11) O2-Sn1-O4* 150.05(11)
[{[$n$$Bu_2$SnOC(O)Fc]$_2$O}$_2$] (**2**) ladder, tetranuclear tetracarboxylate	isobidentate bridging and anisobidentate chelating five-coordinate (2C, 3O) distorted trigonal bipyramidal geometry	Sn1–O2 2.243(2) Sn2–O3 2.249(2) Sn2–O4 2.201(2) Sn2–O5 2.646(3) Sn1–O4 2.768(3)	Sn1–O1 2.168(2) Sn2–O1 2.024(2) Sn1–O1* 2.036(2)	O1-Sn1-O2 167.59(7) O1*-Sn1-C23 106.70(9) O1*-Sn1-C27 108.81(3) C23-Sn1-C27 144.36(11) O3-Sn2-O4 172.05(7) O1-Sn2-C35 110.32(9) O1-Sn2-C31 103.69(9) C31-Sn2-C35 145.32(10) Sn1-O1-Sn2 119.87(8) Sn1*-O1-Sn2 135.70(9)
[$n$$Bu_2$Sn{OC(O)Fc}$_2$] (**3**) mononuclear dicarboxylate	anisobidentate chelating six-coordinate (2C, 4O) skewed trapezoidal bipyramidal geometry	Sn1–O1 2.571(3) Sn1–O2 2.108(3) Sn1–O3 2.116(3) Sn1–O4 2.539(4) Sn2–O5 2.559(3) Sn2–O6 2.127(3) Sn2–O7 2.135(3) Sn2–O8 2.497(3)		C45-Sn1-C49 145.0(3) O2-Sn1-O3 82.41(2) O1-Sn1-O4 166.93(2) C53-Sn2-C57 146.60(2) O6-Sn2-O7 84.87(2) O5-Sn2-O8 164.55(2)
[{$t$$Bu_2$Sn(OH)OC(O)Fc}$_2$] (**4**) dihydroxy-bridged dinuclear dicarboxylate	monodentate five-coordinate (2C, 3O) distorted trigonal bipyramidal geometry	Sn1–O2 2.155(16)	Sn1–O1 2.036(18) Sn1–O1* 2.173(18)	O2-Sn1-O1* 154.55(7) O1-Sn1-C1 117.52(10) O1-Sn1-C5 118.94(9) C1-Sn1-C5 123.45(11) O1-Sn1-O1* 69.77(8) O1-Sn1-O2 85.05(7)
[Ph_3SnOC(O)Fc] (**6**) mononuclear monocarboxylate	anisobidentate chelating five-coordinate (3C, 2O) distorted trigonal bipyramidal geometry	Sn1–O1 2.079(2) Sn1–O2 2.598(2)		C1-Sn1-O1 97.43(6) C1-Sn1-C7 106.00(7) C1-Sn1-C13 111.27(7) C7-Sn1-O1 113.78(6) C7-Sn1-C13 123.56(7) C13-Sn1-O1 101.82(6)

[a] For atom labeling scheme, see Figure 1.

bonds to three phenyl groups and one carboxylate oxygen atom. The other carboxylate oxygen atom undergoes a fifth weaker bonding interaction to the tin atom along the tetrahedral face. Accordingly, two types of Sn–O distances are found for each molecule (Sn1–O1 2.080(2) and Sn1–O2 2.598(2) Å). The geometry around tin may be described as distorted tetrahedral (or capped tetrahedral).

Supramolecular interactions in compounds 1–4 and 6: In recent years there has been considerable interest in organometallic crystal engineering.[8,17] Compounds **1–4** and **6** provide a unique opportunity to understand the nature of supramolecular interactions in a closely related family of organometallic compounds. The presence of the carboxylate oxygen atoms and the cyclopentadienyl C–H groups in **1–4** and **6** allows their organization into intricate supramolecular structures in the solid state. This is assisted (mainly) by C–H···O and π–π interactions. The driving force for the extensive supramolecular interactions arises from many factors. The cyclopentadienyl rings in unsubstituted ferrocene are electron rich, but in ferrocene carboxylates the electron density in the cyclopentadienyl rings is depleted. This promotes the donor capability of the proton and enhances the ability of such units to participate in hydrogen bonding. A summary of the possible ferrocenyl-based supramolecular building blocks is shown in Scheme 5. Unlike simple aromatic compounds, there are only very few reports on interferrocenyl π–π interactions.[8,17] The metric parameters involved in the supramolecular interactions of compounds **1–4** and **6** are given in the Supporting Information. The supramolecular organization will only be described here for compounds **1** and **6** (see Supporting Information for a description of the other compounds). A summary of the supramolecular architectures found in **1–4** and **6** is given in Table 2.

Compound **1** forms an interesting supramolecular assembly in the solid state mediated by weak hydrogen bonds and π-stacking interactions. The overall supramolecular organization may be analyzed in a step-wise manner to facilitate a

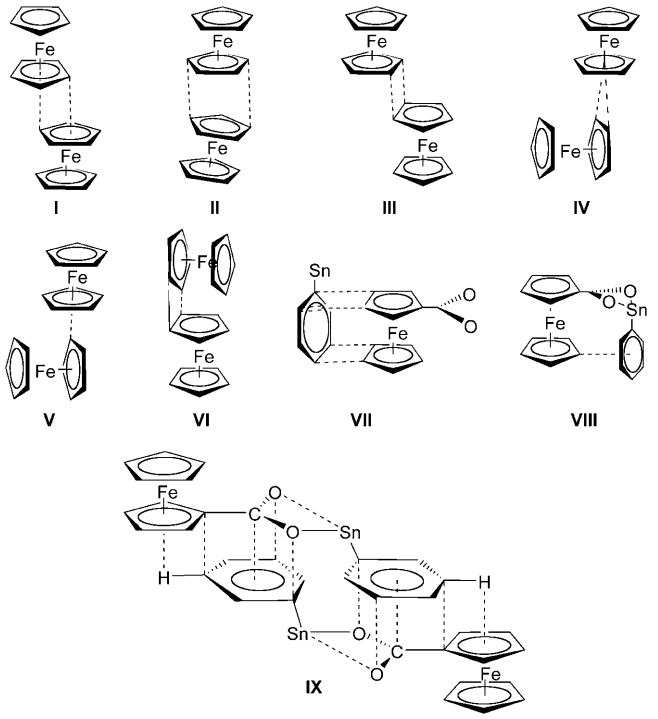

Scheme 5. Summary of the possible ferrocenyl based supramolecular building blocks. Types I and II: parallel displaced stacking; Type III: edge-to-edge stacking; Type IV: T-shaped stacking (edge-to-face); Type V: C–H···π interaction; Type VI: L-shaped stacking (edge-to-edge); Type VII: side-to-face stacking; Type VIII: intramolecular C–H···π interaction; Type IX: C-CO_2–π stacking.

ready understanding. Thus, at the first level of the supramolecular arrangement each planar $Sn_2C_2O_4$ core containing four ferrocene moieties interacts with two other neighboring ladders by means of four proton acceptor–donor type of C–H···O interactions. In this interaction two protons (H17 and H23) of two different ferrocene moieties are intermolecularly hydrogen-bonded to the oxygens (O3 and O2) of the carboxylates of the neighboring two molecules. The resultant C–H···O contacts allow the molecule to arrange into a *staircase* type of one-dimensional linear polymeric array in the solid state (Figure 2A). The distances of the C–H···O interactions are H17···O3 2.536(9) and H23···O2 2.543(7) Å. At the second level of supramolecular assembly, two such one-dimensional staircase networks are interconnected by means of π–π stacking interactions (Type III, Scheme 5) between the cyclopentadienyl groups (C25–C29) to form a double-directional staircase sheet (Figure 2A). The two cyclopentadienyl units involved in this π–π stacking are staggered with an interplanar distance of 3.387(3) Å. Finally, the ferrocenyl π–π dimers present in the two-dimensional sheets are further π-stacked (Type III, Scheme 5) to form a three-dimensional pillared network (Figure 2B). The interplanar distance in these interacting cyclopentadienyl units is 3.478(2) Å (C14–C18 and C30–C34), and their orientation is also staggered. The pillared structure is built from four ferrocenyl groups (Figure 2C) and all the pillars are interconnected through the $Sn_2C_2O_4$ cyclic core. As a result, the overall structure contains long channels (6.5×13.3 Å; Figure 2D). In addition to the above discussed interactions, a T-shaped stacking (Type IV, Scheme 5) is also found between a ferrocenyl group (C30–C34) and one phenyl group (C7–C12). The supramolecular organization of **2** occurs analogously to that of **1**, also leading to the formation of a three-dimensional pillared structure (see Supporting Information).

A closer look at the structure of **3** revealed that the two molecules present in the asymmetric unit interact with two other molecules over long range Sn–O distances (Sn1–O1 2.991(4) Å and Sn2–O6 3.047(6) Å) to afford dimers containing a distannoxane (Sn_2O_2) core. Such Sn–O distances have also been recently observed by Höpfl and co-workers in their studies on dimethyltin phthalates.[11e] It may be noted here that the sum of the van der Waals radii of tin and oxygen is 3.7 Å.[18] Compound **3** forms a double-directional staircase type of polymeric sheet by means of C–H···O interaction. These two-dimensional sheets are further interconnected by four L-shaped π-stacking interactions (Type VI, Scheme 5) to form a three-dimensional architecture. Supramolecular formation in **4** results primarily from intermolecular C–H···O contacts. Additional T-shaped edge-to-face stacking between cyclopentadienyl units represents the secondary interaction (Type IV, Scheme 5). Two helical networks with an opposed screw sense interact with each other to afford a three-dimensional tubular network.

Table 2. Summary of supramolecular interactions in the structures **1**–**4** and **6**.

Compound	Type of interactions	Supramolecular assembly	Remarks
1	intramolecular C–H···π (Type VIII)[a] and π–π intermolecular C–H···π, C–H···O and π–π (Type III and IV)[a]	three-dimensional pillared network	Figures S6[b] and 2
2	intermolecular C–H···O and π–π (Type II and III)[a]	three-dimensional pillared network	Figure S7[b]
3	intermolecular Sn–O contacts intermolecular C–H···O and π–π (VI)[a]	three-dimensional supramolecular network	Figure S8[b]
4	intermolecular C–H···O and π–π (Type IV)[a]	helical three-dimensional tubular network	Figure S9[b]
6	intramolecular C–H···π (Type VIII)[a] intermolecular CO_2–π interaction (Type IX)[a] intermolecular C–H···π, C–H···O and π–π (Type VII)[a]	two-dimensional grid type network	Figures S10[b] and 3

[a] See Scheme 5. [b] See Supporting Information.

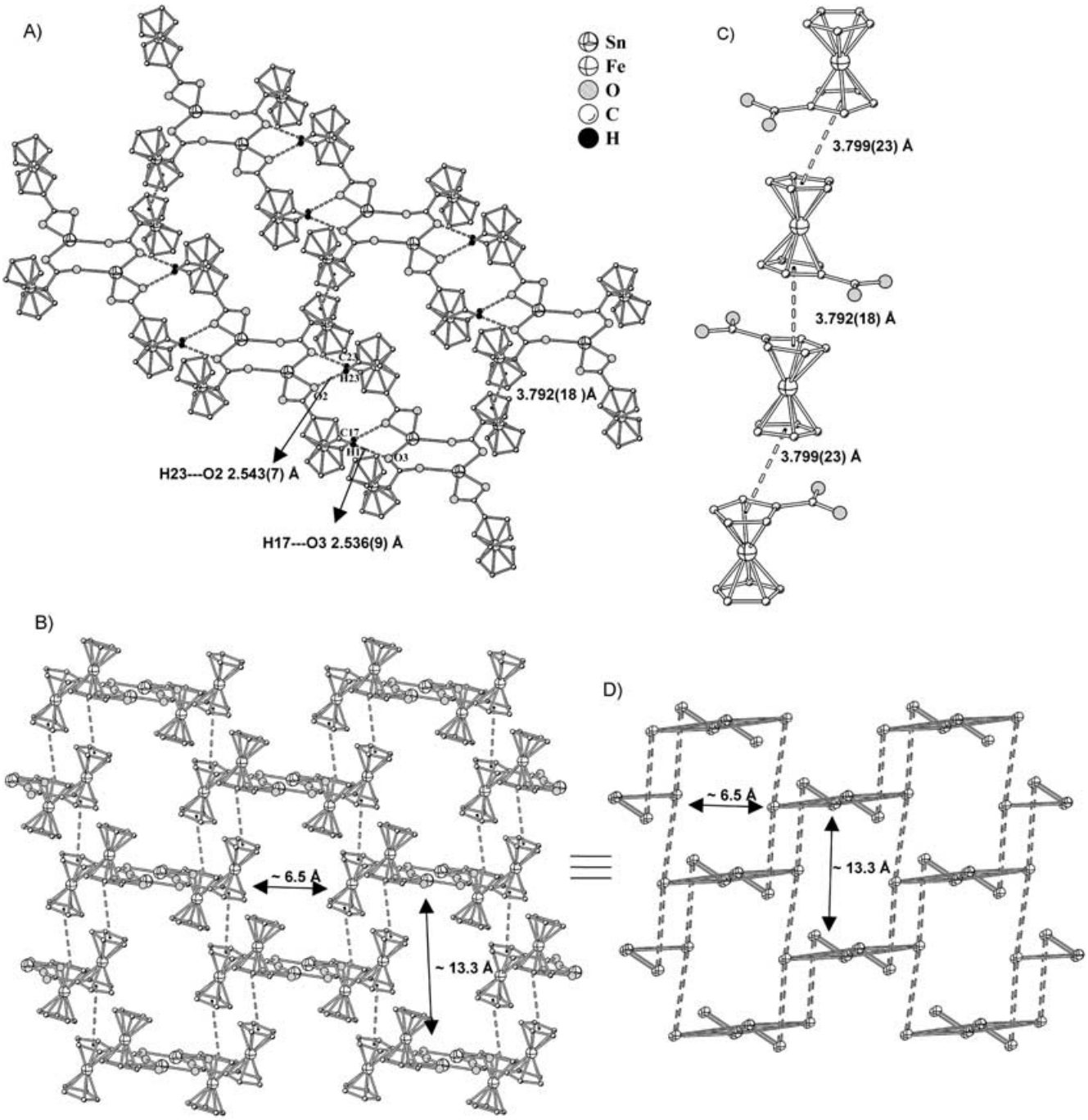

Figure 2. Three-dimensional Supramolecular architecture of **1** arising from of C–H···O and π-stacking interactions. A) View showing the double-directional stair-case type two-dimensional sheet (C–H···O and π–π interactions are shown). B) View showing the three-dimensional pillared network with pore dimensions of 6.5×13.3 Å (C–H···O and π–π interactions are shown). C) Orientation of the ferrocenyl carboxylate groups in each pillar (π–π interactions are shown). D) Cartoon representation of the three-dimensional pillared network shown in B.

The supramolecular network of **6** shows an unprecedented $CpCO_2$-π building block. Two molecules are intermolecularly connected through this interaction (Type IX, Scheme 5), in which the carboxylate carbon atom is positioned right on the top of the centroid of a phenyl group (Figure 3A and 3B; the interplanar distance between O_2C and the phenyl group is 3.695(1) Å with a tilt angle of 9.29°).[19] The ferrocenyl carboxylate group, which participates in the $CpCO_2$-π interaction, is also involved in a side-to-face interaction (Type VII, Scheme 5) with the phenyl group (C22–C23, C27–C28, and C13–C18) present in the neighboring molecule (Figure 3A). Interplanar distances of this interaction are 3.732(1) Å. In addition, C–H···O contacts between the carboxylate oxygen atom and a phenyl C–H group are also

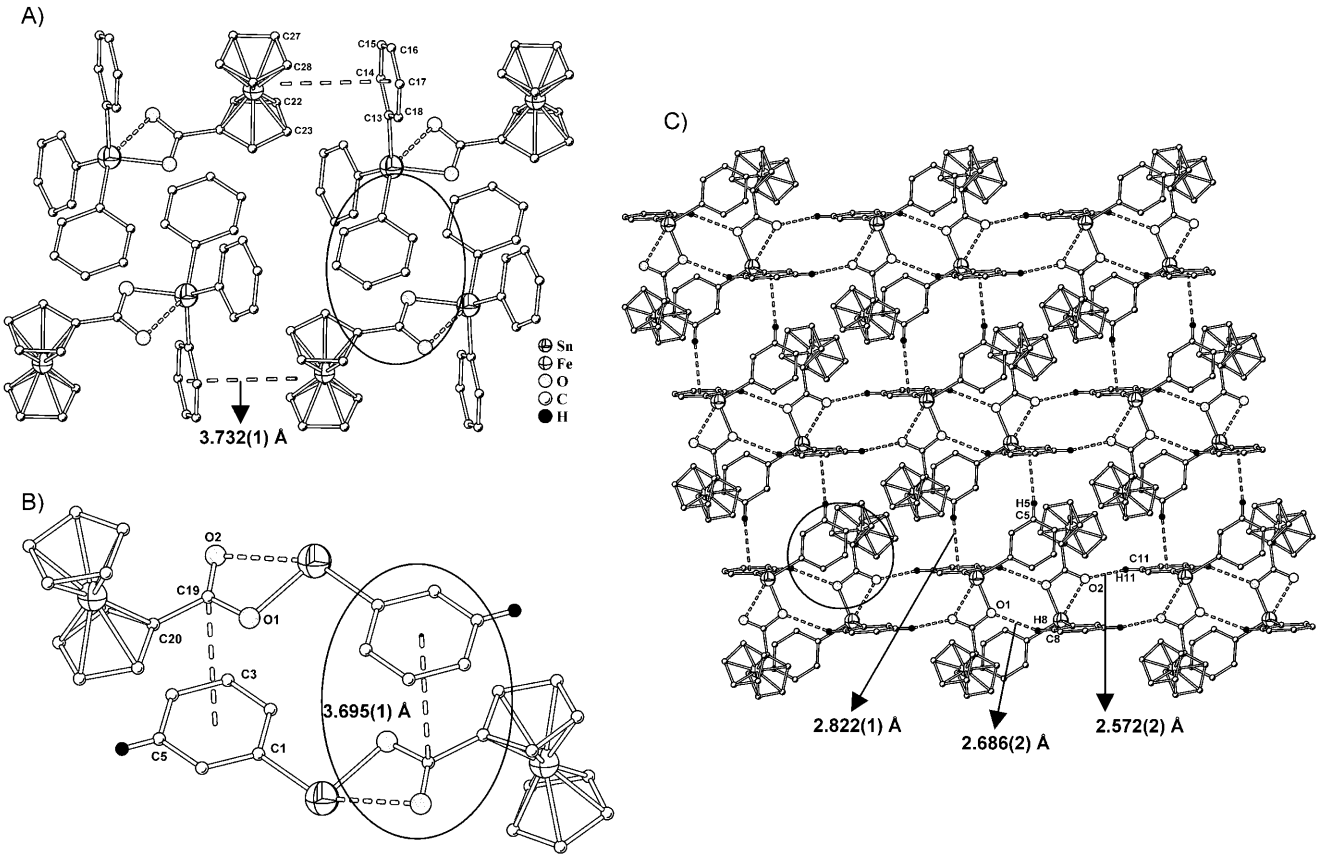

Figure 3. CO_2–π stacking, C–H···O, and C–H···π interactions assisted supramolecular assembly of **6**. In all the figures the inset circle shows CO_2–π stacking interaction. A) View showing the CO_2–π stacking interaction as well as side-to-face stacking between phenyl and ferrocenyl groups. B) Orientation of the CO_2–π stacking interactions. C) Two-dimensional supramolecular network arising from of C–H···O and C–H···π interactions.

present (H8···O1 2.686(2) and H11···O2 2.572(2) Å). These two types of weak secondary interactions lead to the formation of one-dimensional tapes (Figure 3C) that are interconnected to each other by C–H···π contacts affording a two dimensional grid (H5···π 2.822(1) Å; Figure 3C).

Electrochemical studies: Electrochemical studies (cyclic and differential pulse voltammetry) on compounds **1**–**7** were carried out. The electrochemical data for these compounds along with some other related derivatives are summarized in Table 3. The compounds **1**–**4**, **6**, and **7** show a single quasi-reversible oxidation similar to that observed for the hexaferrocenyl derivative $[\{n\text{BuSn(O)OC(O)Fc}\}_6]$.[4a] This behavior suggests that although in the solid state there are differences in the orientations of the ferrocenyl groups, in solution they behave in an equivalent manner. Furthermore, the peak potentials at which oxidation occurs are nearly invariant and do not seem to depend upon the nature of the organotin assembly. This confirms the suggestion that organotin assemblies can be utilized as redox-inactive scaffolds for supporting redox-active peripheries. A representative example of the electrochemical behavior of these compounds is illustrated by Figure 4, which shows the cyclic and differential pulse voltammograms of compound **2** (see Supporting Information for cyclic voltammetric traces of the other compounds). Interestingly, although the tin assembly does not influence the peak potentials of the appended ferrocene units, there appears to be an influence on the electrochemical stability in solution. Thus, **2** and **4**, which possess a central Sn_2O_2 core, do not show electrochemical decomposition in solution even after ten continuous CV cycles. In contrast, compounds **1**, **3**, and **5**–**7** slowly start to decompose after the fifth cycle. It

Table 3. Cyclic voltammetric data for compounds **1**–**7** along with some other multiferrocene derivatives.

Compound	$E_{1/2}$ [V][a]	ΔE_p [mV]	References
$[(Cp)FeC_6\{(CH_2)_5Fc\}_6]PF_6$	+0.44	55	[20]
$[C_6\{(CH_2)_5Fc\}_6]$	+0.45	–	[20]
$[CpFeC_6\{(CH_2)_2C_6H_4OC(O)Fc\}_6]PF_6$	+0.78	60	[21]
$[C_6\{(CH_2)_2C_6H_4OC(O)Fc\}_6]$	+0.88	120	[21]
$[\{n\text{BuSn(O)OC(O)Fc}\}_6]$	+0.72	128	[4a]
$[\{n\text{BuSn(O)OC(O)CH}_2\text{Fc}\}_6]$	+0.50	240	[4b]
$[\{Ph_2Sn[OC(O)Fc]_2\}_2]$ (**1**)	+0.69	105	this work
$[\{[n\text{Bu}_2\text{SnOC(O)Fc}]_2O\}_2]$ (**2**)	+0.73	184	this work
$[n\text{Bu}_2\text{Sn}\{OC(O)Fc\}_2]$ (**3**)	+0.70	158	this work
$[\{t\text{Bu}_2\text{Sn(OH)OC(O)Fc}\}_2]$ (**4**)	+0.69	246	this work
$[t\text{Bu}_2\text{Sn}\{OC(O)Fc\}_2]$ (**5**)	+0.65	105	this work
	+0.74	92	
$[Ph_3SnOC(O)Fc]$ (**6**)	+0.66	106	this work
$[\{n\text{Bu}_3\text{SnOC(O)Fc}\}_n]$ (**7**)	+0.57	112	this work

[a] Versus SCE; $Fc = (C_5H_4)Fe(C_5H_5)$.

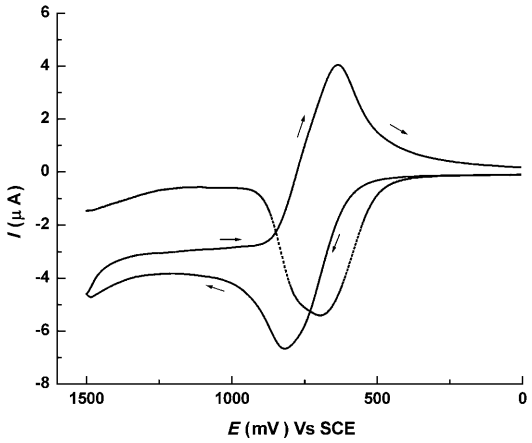

Figure 4. Cyclic (CV) and differential pulse (DPV) voltammogram of the tetraferrocenyl assembly **2**.

may be noted that the hexaferrocenyl derivative [{*n*BuSn(O)OC(O)Fc}$_6$][4a], which also contains the Sn_2O_2 motifs, is electrochemically stable. The electrochemical behavior of **5** shows two quasi-reversible oxidation peaks. We attribute this to the structural difference of the compound in the form of a varying coordination behavior of the ferrocene units. We propose that one of the ferrocene moieties coordinates in an anisobidentate mode, while the other is monodentate (Scheme 3). This proposal has to await a structural confirmation. We have so far been unable to obtain suitable single crystals of **5**.

Conclusion

The Sn−O bond formation reaction can be utilized for decorating the stannoxane assemblies with varied and interesting groups. We have shown that this approach can be utilized to assemble compounds containing six, four, two, and one ferrocenyl units. The synthetic method for organostannoxane assemblies ensures nearly quantitative yields. Interestingly, both solid-state and solution synthetic methodologies are applicable. The X-ray crystal structure analysis of these compounds revealed an unprecedented structural form of an organotin carboxylate (compound **1**). A detailed examination of the crystal structures of all of these compounds showed a rich supramolecular organization facilitated by C−H···O contacts and augmented by π–π interactions. We have also observed T- and L-stacking as well as C−H···π interactions. The cumulative effect of these varied weak contacts is to generate two- and three-dimensional supramolecular architectures were generated. The crystal engineering principles deduced from these interactions appear to be fairly general and reproducible. The electrochemical behavior of the stannoxane-supported ferrocenyl derivatives illustrates that the stannoxane motifs are electrochemically inert and can be utilized as platforms for building multiple redox-active assemblies. The electrochemical stability of these compounds is enhanced by the presence of robust stannoxane cores that are built from Sn_2O_2 units.

Experimental Section

Reagents and general procedures: All operations were carried out in an atmosphere of nitrogen or argon. Solvents were freshly distilled over suitable drying agents. $(Ph_2SnO)_n$, $(nBu_2SnO)_n$, $(Ph_3Sn)_2O$, $(nBu_3Sn)_2O$, and FcCOOH (Fc = $\eta^5C_5H_4$-Fe-$\eta^5C_5H_5$) (Aldrich) were purchased and used without further purification. $(tBu_2SnO)_3$ was prepared according to a literature procedure.[22]

Instrumentation: Melting points were recorded using a JSGW melting point apparatus and are uncorrected. Elemental analyses were carried out using a Thermoquest CE instruments model EA/110 CHNS-O elemental analyzer. ^{1}H and ^{119}Sn NMR spectra were obtained on a JEOL-JNM LAMBDA 400 model spectrometer with $CDCl_3$ as the solvent. The chemical shifts are referenced with respect to tetramethylsilane (^{1}H) and tetramethyltin (^{119}Sn). All the ^{119}Sn NMR spectra were recorded under broadband decoupled conditions. FAB mass spectra were recorded on a JEOL SX 102/DA-6000 mass spectrometer with argon/xenon (6 kV, 10 mA) as the FAB gas. The accelerating voltage was 10 kV, and the spectra were recorded at room temperature. Cyclic voltammetric experiments were carried out on an EG&G Princeton Applied Research model 273 A Polarographic Analyzer by using a three-electrode configuration of a platinum working electrode, a commercially available saturated calomel electrode (SCE) as the reference electrode, and a platinum mesh electrode. Half-wave potentials were measured as the average of the cathodic and anodic peak potentials. The voltammograms were recorded in CH_2Cl_2 containing 0.1 M Bu_4NPF_6 as the supporting electrolyte and the potential was scanned from 0 to +1.8 V at various scan rates.

The general synthetic procedure for the preparation of the various ferrocenyl compounds (1–7): A stoichiometric mixture of the organotin precursor and ferrocene carboxylic acid in toluene (70 mL) was heated under reflux for 6 h. The water formed in the reaction was removed by using a Dean–Stark apparatus. The reaction mixture was filtered and evaporated to afford the corresponding products, which were purified subsequently by recrystallization.

Compounds **1–7** were also prepared by a solvent-free strategy. Briefly, this method consisted of grinding a stoichiometric mixture of the organotin precursor and the ferrocene carboxylic acid for a time range between 15 and 45 min. At the completion of the grinding period the product was extracted with CH_2Cl_2 and crystallized.[10] The stoichiometric ratio of the reactants, the yields, and the characterization data of the products **1–7** are given below.

[{$Ph_2Sn[OC(O)Fc]_2$}$_2$] (1): In 1:1 ratio: Ph_2SnO (0.29 g, 1.0 mmol), FcCOOH (0.23 g, 1.0 mmol), yield: 0.34 g (65.9 %); solvent-free method: Ph_2SnO (0.06 g, 0.2 mmol), FcCOOH (0.05 g, 0.2 mmol), grinding time: 45 min, yield: 0.06 g (59.5 %). In 1:2 ratio: Ph_2SnO (0.17 g, 0.6 mmol), FcCOOH (0.28 g, 1.2 mmol), yield: 0.42 g (96.1 %); solvent-free method: Ph_2SnO (0.04 g, 0.15 mmol), FcCOOH (0.07 g, 0.3 mmol), grinding time: 45 min, yield: 0.11 g (98.8 %); m.p. 212 °C; elemental analysis calcd (%) for $C_{68}H_{56}O_8Fe_4Sn_2$: C 55.86, H 3.86; found: C 54.94, H 3.95; ^{1}H NMR δ = 3.85 (s, 10 H; ferrocenyl), 4.48 (s, 8 H; ferrocenyl), 7.52 (d, J = 8.03 Hz, 4 H; phenyl), 7.92 (d, J = 8.03 Hz, 2 H; phenyl), 8.14 ppm (s, 4 H; phenyl); ^{119}Sn NMR δ = −321.4 ppm (s).

[{[$n$$Bu_2$SnOC(O)Fc]$_2$O}$_2$] (2): nBu_2SnO (0.50 g, 2.0 mmol), FcCOOH (0.46 g, 2.0 mmol), yield: 0.85 g (90.1 %); solvent-free method: nBu_2SnO (0.10 g, 0.4 mmol), FcCOOH (0.09 g, 0.4 mmol), grinding time: 45 min, yield: 0.18 g (95.8 %); m.p. 136–137 °C; elemental analysis calcd (%) for $C_{76}H_{108}O_{10}Sn_4Fe_4$: C 48.56, H 5.79; found: C 48.93, H 5.13; ^{1}H NMR δ = 0.87 (t, J = 7.2 Hz, 3 H; butyl methyl), 1.18–1.72 (m, 6 H; butyl CH_2), 4.17–4.67 ppm (m, 9 H; ferrocenyl); ^{119}Sn NMR δ = −215.9 (s), −222.0 ppm (s).

[$n$$Bu_2$Sn{OC(O)Fc}$_2$] (3): nBu_2SnO (0.44 g, 1.75 mmol), FcCOOH (0.81 g, 3.50 mmol), yield: 1.18 g (98.9 %); solvent-free method: nBu_2SnO

(0.07 g, 0.3 mmol), FcCOOH (0.14 g, 0.6 mmol), grinding time: 45 min, yield: 0.19 g (92.7%); m.p. 152°C; elemental analysis calcd (%) for $C_{30}H_{36}O_4Fe_2Sn$: C 52.14, H 5.25; found: C 52.68, H 5.0; MS: *m/z* (%): 692 $[M+1]^+$ (36); ^{1}H NMR $\delta = 0.87$ (t, $J = 7.34$ Hz, 3H; butyl methyl), 1.34–1.38 (h, $J = 7.2$ Hz, 2H; butyl CH_2), 1.68–1.73 (m, 4H; butyl CH_2), 4.18 (s, 5H; ferrocenyl), 4.37 (s, 2H; ferrocenyl), 4.82 ppm (s, 2H; ferrocenyl); ^{119}Sn NMR $\delta = -158.6$ ppm (s).

[{*t*Bu$_2$Sn(OH)OC(O)Fc}$_2$] (4): (tBu$_2$SnO)$_3$ (0.22 g, 0.3 mmol), FcCOOH (0.21 g, 0.9 mmol), yield: 0.39 g (90.3%); solvent-free method: (tBu$_2$SnO)$_3$ (0.03 g, 0.04 mmol), FcCOOH (0. 028 g, 0.12 mmol), grinding time: 15 min, yield: 0.051 g (88.7%); m.p. 202°C; elemental analysis calcd (%) for $C_{38}H_{56}O_6Sn_2Fe_2$: C 47.64, H 5.89; found: C 47.41, H 5.01; ^{1}H NMR $\delta = 1.39$ (s, 36H; butyl methyl), 4.13 (s, 10H; ferrocenyl), 4.25 (s, 4H; ferrocenyl), 4.68 (s, 4H; ferrocenyl), 7.83 ppm (s, 2H; hydroxyl); ^{119}Sn NMR $\delta = -271.1$ ppm (s).

[*t*Bu$_2$Sn{OC(O)Fc}$_2$] (5): (tBu$_2$SnO)$_3$ (0.15 g, 0.2 mmol), FcCOOH (0.28 g, 1.2 mmol), yield: 0.41 g (97.3%); solvent-free method: (tBu$_2$SnO)$_3$ (0.015 g, 0.02 mmol), FcCOOH (0.028 g, 0.12 mmol), grinding time: 15 min, yield: 0.039 g (94.1%); m.p. 241°C; elemental analysis calcd (%) for $C_{30}H_{36}O_4Fe_2Sn$: C 52.14, H 5.25; found: C 52.68, H 5.01; ^{1}H NMR $\delta = 1.41$ (s, 18H; butyl methyl), 4.21 (s, 10H; ferrocenyl), 4.34 (s, 4H; ferrocenyl), 4.80 ppm (s, 4H; ferrocenyl); ^{119}Sn NMR $\delta = -213.2$ ppm (s).

[Ph$_3$SnOC(O)Fc] (6): $(Ph_3Sn)_2O$ (0.72 g, 1.0 mmol), FcCOOH (0.46 g, 2.0 mmol), yield: 1.05 g (89.7%); solvent-free method: $(Ph_3Sn)_2O$ (0.14 g, 0.2 mmol), FcCOOH (0.09 g, 0.4 mmol), grinding time: 30 min, yield: 0.22 g (95.0%); m.p. 105°C; elemental analysis calcd (%) for $C_{29}H_{24}O_2SnFe$: C 60.15, H 4.18; found: C 60.89, H 4.27; MS: *m/z* (%): 579 $[M]^+$ (100); ^{1}H NMR $\delta = 3.99$ (s, 5H; ferrocenyl), 4.35 (t, $J = 1.96$ Hz, 2H; ferrocenyl), 4.84 (t, $J = 1.96$ Hz, 2H; ferrocenyl), 7.45–7.47 (m, 9H; phenyl), 7.80–7.82 ppm (m, 6H; phenyl); ^{119}Sn NMR $\delta = -117.9$ ppm (s).

[{*n*Bu$_3$SnOC(O)Fc}$_n$] (7): (nBu$_3$Sn)$_2$O (0.36 g, 0.6 mmol), FcCOOH (0.28 g, 1.2 mmol), yield: 0.62 g (99.2%); solvent-free method: (nBu$_3$Sn)$_2$O (0.12 g, 0.2 mmol), FcCOOH (0.09 g, 0.4 mmol), grinding time: 15 min, yield: 0.20 g (97.0%); m.p. 98°C; elemental analysis calcd (%) for $C_{23}H_{36}O_2SnFe$: C 53.22, H 6.99; found: C 53.01, H 6.18; ^{1}H NMR $\delta = 0.86$ (t, $J = 7.31$ Hz, 9H; butyl CH_3), 1.60–1.24 (m, 18H; butyl CH_2), 4.10 (s, 5H; ferrocenyl), 4.25 (t, $J = 1.96$ Hz, 2H; ferrocenyl), 4.68 ppm (t, $J = 1.95$ Hz, 2H; ferrocenyl); ^{119}Sn NMR $\delta = 102.9$ ppm (s).

X-ray crystal structure determination of 1–4 and 6: Single crystals of **1** were obtained from the reaction mixture at room temperature. Single crystals of **3** were obtained by vapor diffusion of *n*-hexane into a solution of compound **3** in $CHCl_3$. X-ray quality crystals for compound **2** were obtained by cooling a solution of **2** in CH_2Cl_2 in a refrigerator at 5°C. Crystals of **4** and **6** were obtained by slow evaporation of solutions of **4** or **6** in CH_2Cl_2 or toluene, respectively. Suitable crystals for single-crystal X-ray diffraction measurements were loaded on a Bruker AXS Smart Apex CCD diffractometer ($\lambda = 0.71073$ Å). All structures were solved by direct methods by using SHELXS-97[23a] or SHELXTL[23b] and refined by full-matrix least squares on F^2 using SHELXL-97.[23a] All hydrogen atoms with occupancy >0.5 were included in idealized positions, and their positions were refined anisotropically by a riding model. Non-hydrogen atoms were refined with anisotropic displacement parameters. Details of the data collection and refinement parameters are given in Table 4.

CCDC-257982 to CCDC-257987 contain the supplementary crystallographic data for this paper. These data can be obtained free of charge from The Cambridge Crystallographic Data Centre via www.ccdc.cam.ac.uk/data_request/cif.

Table 4. Crystal data collection and refinement parameters for **1**–**4** and **6**.

	1	**2**	**3**	**4**	**6**
formula	$C_{34}H_{28}O_4SnFe_2$	$C_{76}H_{108}O_{10}Sn_4Fe_4$	$C_{68}H_{92}O_8Sn_2Fe_4$	$C_{38}H_{56}O_6Sn_2Fe_2$	$C_{29}H_{24}O_2SnFe$
M_r	730.95	1879.78	1498.20	957.91	579.02
T [K]	100(2)	150(2)	298(2)	213(2)	100(2)
crystal system	triclinic	triclinic	triclinic	tetragonal	triclinic
space group	$P\bar{1}$	$P\bar{1}$	$P\bar{1}$	$I4_1/a$	$P\bar{1}$
a [Å]	10.930(3)	12.1760(6)	13.875(2)	22.1550(2)	9.9536(6)
b [Å]	11.298(3)	13.8717(7)	15.944(3)	22.1550(2)	11.2191(7)
c [Å]	13.019(4)	13.9010(7)	16.481(3)	16.448(2)	11.5985(7)
α [°]	102.164(5)	63.7040(10)	86.298(3)	90	98.4910(10)
β [°]	110.315(5)	64.8980(10)	67.159(3)	90	106.2580(10)
γ [°]	106.755(5)	73.6100(10)	65.609(3)	90	105.5420(10)
V [Å^3]	1354.5 (7)	1893.25 (16)	3040.1 (9)	8073.5(16)	1162.71(12)
Z	2	1	2	8	2
ρcalcd [mg m^{-3}]	1.792	1.649	1.637	1.576	1.654
μ [mm^{-1}]	2.012	2.095	1.795	1.969	1.722
F(000)	732	948	1536	3872	580
crystal size [mm^3]	0.5×0.5×0.2	0.5×0.4×0.3	0.5×0.3×0.3	0.4×0.4×0.3	0.3×0.3×0.2
θ range [°]	2.01–28.36	1.65–28.29	2.50–28.59	1.84–24.03	1.88–28.28
limiting indices	$-14 \le h \le 11$	$-7 \le h \le 16$	$-18 \le h \le 18$	$-25 \le h \le 25$	$-13 \le h \le 13$
	$-14 \le k \le 15$	$-18 \le k \le 18$	$-21 \le k \le 21$	$-25 \le k \le 24$	$-10 \le k \le 14$
	$-16 \le l \le 17$	$-16 \le l \le 18$	$-14 \le l \le 21$	$-18 \le l \le 18$	$-15 \le l \le 15$
reflections collected	9029	12053	20509	17632	14202
independent reflections	6426	8386	14534	3156	5697
	[R(int) = 0.0409]	[R(int) = 0.0170]	[R(int) = 0.0196]	[R(int) = 0.0607]	[R(int) = 0.0181]
completeness to θ [%]	94.7	89.1	93.5	99.3	98.7
Absorption correction	Bruker SADABS	Semi-empirical	Bruker SADABS	None	Bruker SADABS
data/restrains/parameters	6426/0/370	8386/60/422	14534/0/695	3156/0/227	5697/0/298
goodness-of-fit on F^2	1.018	1.027	1.051	0.973	1.050
final R indices [$I > 2\sigma(I)$]	$R1 = 0.0489$,	$R1 = 0.0283$,	$R1 = 0.0504$,	$R1 = 0.0210$,	$R1 = 0.0234$,
	$wR2 = 0.1202$	$wR2 = 0.0669$	$wR2 = 0.1395$	$wR2 = 0.0499$	$wR2 = 0.0570$
R indices (all data)	$R1 = 0.0606$,	$R1 = 0.0343$,	$R1 = 0.0681$,	$R1 = 0.0260$,	$R1 = 0.0249$,
	$wR2 = 0.1268$	$wR2 = 0.0699$	$wR2 = 0.1528$	$wR2 = 0.0511$	$wR2 = 0.0578$
largest diff peak/hole [e Å^{-3}]	1.467/−0.687	0.873/−0.481	1.344/−0.783	0.316/−0.273	0.960/−0.459

$R = \Sigma ||F_o| - |F_c|| / \Sigma |F_o|$; $wR = \{[\Sigma w(|F_o|^2 - |F_c|^2)^2] / [\Sigma w(|F_o|^2)^2]\}^{1/2}$.

The asymmetric units of **1** and **4** contain half a molecule of the cluster with one tin atom (Sn1). The asymmetric unit of **2** contains half a molecule of the cluster with two tin atoms (Sn1 and Sn2). Four carbon atoms in two different *n*-butyl groups (C26, C28–C30) are disordered over two orientations and are labeled C26 and C26′, C28 and C28′, C29 and C29′, C30 and C30′ with a 0.75:0.25 occupancy ratio. These were refined isotropically. The asymmetric unit of **3** contains two molecules and one hexane molecule as a solvate. The carbon atoms in the hexane molecule are disordered, were refined isotropically, and their protons are not included. The proton (H1O) of the bridged hydroxyl group in **4** was included from the electron density map and refined isotropically. The asymmetric unit of **6** contains a single molecule with one tin atom (Sn1).

Acknowledgements

We thank the Department of Science and Technology (India) for financial support including the support for a CCD X-ray facility at IIT-Kanpur. K.G., S.N., and P.S. thank the Council of Scientific and Industrial Research (India) for Senior and Junior Research Fellowships, respectively. A.S., S.Z., and J.F.B. thank the EPSRC (UK) for financial support. We thank Prof. T. K. Chandrasekhar, V. Prabhu Raja, Dr. J. K. Bera and S. K. Patra, Department of Chemistry, Indian Institute of Technology, Kanpur, for their assistance in electrochemical studies.

[1] a) J. B. Flanagan, S. Margel, A. J. Bard, F. C. Anson, *J. Am. Chem. Soc.* **1978**, *100*, 4248–4253; b) J. C. Medina, T. T. Goodnow, S. Bott, J. L. Atwood, A. E. Kaifer, G. W. Gokel, *J. Chem. Soc. Chem. Commun.* **1991**, 290–292; c) D. Astruc, *Acc. Chem. Res.* **1997**, *30*, 383–391; d) C. Valério, J.-L. Fillaut, J. Ruiz, J. Guittard, J.-C. Blais, D. Astruc, *J. Am. Chem. Soc.* **1997**, *119*, 2588–2589; e) F. Frehill, K. H. G. Schulte, C. P. Martin, L. Wang, S. Patel, J. A. Purton, J. G. Vos, P. Moriarty, *Langmuir* **2004**, *20*, 6421–6429; f) P. A. Chase, R. J. M. K. Gebbink, G. van Koten, *J. Organomet. Chem.* **2004**, *689*, 4016–4054, and references therein.

[2] a) A. J. Bard, *Nature* **1995**, *374*, 13; b) K. Takada, D. J. Dýaz, H. D. Abruña, I. Cuadrado, C. Casado, B. Alonso, M. Morán, J. Losada, *J. Am. Chem. Soc.* **1997**, *119*, 10763–10773; c) P. D. Beer, *Acc. Chem. Res.* **1998**, *31*, 71–80; d) D. Astruc, *Acc. Chem. Res.* **2000**, *33*, 287–298; e) S. Nlate, J. Ruiz, V. Sartor, R. Navarro, J.-C. Blais, D. Astruc, *Chem. Eur. J.* **2000**, *6*, 2544–2553.

[3] a) I. Cuadrado, M. Morán, C. M. Casado, B. Alonso, F. Lobete, B. Garcýa, M. Ibisate J. Losada, *Organometallics* **1996**, *15*, 5278–5280; b) I. Cuadrado, C. M. Casado, B. Alonso, M. Morán, J. Losada, V. Belsky, *J. Am. Chem. Soc.* **1997**, *119*, 7613–7614; c) C. Valério, E. Alonso, J. Ruiz, J.-C. Blais, D. Astruc, *Angew. Chem.* **1999**, *111*, 1855–1859; *Angew. Chem. Int. Ed.* **1999**, *38*, 1747–1751; d) S. Nlate, J. Ruiz, J.-C. Blais, D. Astruc, *Chem. Commun.* **2000**, 417–418; e) C. O. Turrin, J. Chiffre, D. de Montauzon, J. C. Daran, A.-M. Caminade, E. Manoury, G. Balavoine J. P. Majoral, *Macromolecules* **2000**, *33*, 7328–7336; f) C. O. Turrin, J. Chiffre, J. C. Daran, D. de-Montauzon, A.-M. Caminade, E. Manoury, G. Balavoine J. P. Majoral, *Tetrahedron* **2001**, *57*, 2521–2536.

[4] a) V. Chandrasekhar, S. Nagendran, S. Bansal, M. A. Kozee, D. R. Powell, *Angew. Chem.* **2000**, *112*, 1903–1905; *Angew. Chem. Int. Ed.* **2000**, *39*, 1833–1835; b) V. Chandrasekhar, S. Nagendran, S. Bansal, A. W. Cordes, A. Vij, *Organometallics* **2002**, *21*, 3297–3300; c) V. Chandrasekhar, G. T. S. Andavan, S. Nagendran, V. Krishnan, R. Azhakar, R. J. Butcher, *Organometallics* **2003**, *22*, 976–986.

[5] a) P. Jutzi, C. Batz, B. Neumann, H.-G. Stammler, *Angew. Chem.* **1996**, *108*, 2272–2274; *Angew. Chem. Int. Ed. Engl.* **1996**, *35*, 2118–2121; b) B. Grossmann, J. Heinze, E. Herdtweck, F. H. Köhler, H. Nöth, H. Schwenk, M. Spiegler, W. Wachter, B. Weber, *Angew. Chem.* **1997**, *109*, 384–386; *Angew. Chem. Int. Ed. Engl.* **1997**, *36*, 387–389; c) N. Prokopuk, D. F. Shriver, *Inorg. Chem.* **1997**, *36*, 5609–5613; d) K. C. K. Swamy, S. Nagabrahmanandachari, K. Raghuraman, *J. Organomet. Chem.* **1999**, *587*, 132–135; e) M. W. Cooke, T. S. Cameron, K. N. Robertson, J. C. Swarts, M. A. S. Aquino, *Organometallics* **2002**, *21*, 5962–5971; f) S. Sengupta, *Tetrahedron Lett.* **2003**, *44*, 7281–7284; g) S. Sengupta, *Polyhedron* **2003**, *22*, 1237–1240; h) S. S. Kumar, N. D. Reddy, H. W. Roesky, D. Vidovic, J. Magull, R. F. Winter, *Organometallics* **2003**, *22*, 3348–3350; i) S. S. Kumar, J. Rong, S. Singh, H. W. Roesky, D. Vidovic, J. Magull, D. Neculai, V. Chandrasekhar, M. Baldus, *Organometallics* **2004**, *23*, 3496–3500; j) G.-L. Zheng, J.-F. Ma, J.-M. Su, L.-K. Yan, J. Yang, Y.-Y. Li, J.-F. Liu, *Angew. Chem.* **2004**, *116*, 2463–2465; *Angew. Chem. Int. Ed.* **2004**, *43*, 2409–2411; k) S. S. Kumar, H. W. Roesky, O. Andronesi, M. Baldus, R. F. Winter, *Inorg. Chim. Acta* **2005**, *358*, 2349–2354.

[6] J. Tao, W. Xiao, Q. Yang, *J. Organomet. Chem.* **1997**, *531*, 223–226.

[7] a) E. A. Meyer, R. K. Castellano, F. Diederich, *Angew. Chem.* **2003**, *115*, 1244–1287; *Angew. Chem. Int. Ed.* **2003**, *42*, 1210–1250; b) H. W. Roesky, M. Andruh, *Coord. Chem. Rev.* **2003**, *236*, 91–119; c) K. Müller-Dethlefs, P. Hobza, *Chem. Rev.* **2000**, *100*, 143–168; d) C. Janiak, *J. Chem. Soc. Dalton Trans.* **2000**, 3885–3896; e) I. Dance, M. Scudder, *Chem. Eur. J.* **1996**, *2*, 481–486; f) G. R. Desiraju, T. Steiner, *The Weak Hydrogen Bond In Structural Chemistry and Biology*, Oxford University Press, Oxford, **1999**.

[8] a) D. Braga, L. Maini, M. Polito, E. Tagliavini, F. Grepioni, *Coord. Chem. Rev.* **2003**, *246*, 53–71; b) D. Braga, F. Grepioni, *Acc. Chem. Res.* **2000**, *33*, 601–608; c) D. Braga, F. Grepioni, *Coord. Chem. Rev.* **1999**, *183*, 19–41; d) K. Mahmoud, Y.-T. Long, G. Schatte, H. B. Kraatz, *J. Organomet. Chem.* **2004**, *689*, 2250–2255.

[9] a) R. R. Holmes, *Acc. Chem. Res.* **1989**, *22*, 190–197; b) E. R. T. Tiekink, *Appl. Organomet. Chem.* **1991**, *5*, 1–23; c) V. K. Jain, *Coord. Chem. Rev.* **1994**, *135*/136, 809–843; d) V. Chandrasekhar, S. Nagendran, V. Baskar *Coord. Chem. Rev.* **2002**, *235*, 1–52.

[10] V. Chandrasekhar, V. Baskar, R. Boomishankar, K. Gopal, S. Zacchini, J. F. Bickley, A. Steiner, *Organometallics* **2003**, *22*, 3710–3716.

[11] a) M. Gielen, A. E. Khloufi, M. Biesemans, F. Kayser, R. Willem, B. Mahieu, D. Maes, J. N. Lisgarten, L. Wyns, A. Moreira, T. K. Chattopadhay, R. A. Palmer, *Organometallics* **1994**, *13*, 2849–2854; b) S. G. Teoh, S. H. Ang, E. S. Looi, C. A. Keok, S. B. Teo, H. K. Fun, *J. Organomet. Chem.* **1997**, *527*, 15–19; c) C. Ma, Q. Jiang, R. Zhang, D. Wang, *Dalton Trans.* **2003**, 2975–2978; d) C. Ma, Q. Jiang, R. Zhang, *Can. J. Chem.* **2004**, *82*, 608–615; e) R. García-Zarracino, J. Ramos-Quiñones, H. Höpfl, *Inorg. Chem.* **2003**, *42*, 3835–3845; f) R. García-Zarracino, H. Höpfl, *Angew. Chem.* **2004**, *116*, 1533–1537; *Angew. Chem. Int. Ed.* **2004**, *43*, 1507–1511; g) R. García-Zarracino, H. Höpfl, *J. Am. Chem. Soc.* **2005**, *127*, 3120–3130.

[12] a) V. Chandrasekhar, V. Baskar, A. Steiner, S. Zacchini, *Organometallics* **2004**, *23*, 1390–1395; b) J. Beckmann, D. Dakternieks, A. Duthie, C. Mitchell, *Organometallics* **2003**, *22*, 2161–2164; c) R. Shankar, M. Kumar, S. P. Narula, R. K. Chadha, *J. Organomet. Chem.* **2003**, *671*, 35–42; d) F. Ribot, C. Sanchez, M. Biesemans, F. A. G. Mercier, J. C. Martins, M. Gielen, R. Willem, *Organometallics* **2001**, *20*, 2593–2603.

[13] S.-G. Teoh, S.-H. Ang, E.-S. Looi, C.-A. Keok, S.-B. Teo, J.-P. Declercq, *J. Organomet. Chem.* **1996**, *523*, 75–78.

[14] H. Puff, H. Heide, H. Kornelia, H. Reuter, S. Willi, *J. Organomet. Chem.* **1985**, *287*, 163–178.

[15] a) V. Chandrasekhar, V. Baskar, A. Steiner, S. Zacchini, *Organometallics* **2002**, *21*, 4528–4532; b) V. Chandrasekhar, V. Baskar, *Indian J. Chem. Sect. A* **2003**, *42*, 2376–2381.

[16] V. B. Mokal, V. K. Jain, E. R. T. Tiekink, *J. Organomet. Chem.* **1992**, *431*, 283–288.

[17] a) S. Masaoka, D. Tanaka, Y. Nakanishi, S. Kitagawa, *Angew. Chem.* **2004**, *116*, 2584–2588; *Angew. Chem. Int. Ed.* **2004**, *43*, 2530–2534; b) D. Braga, L. Maini, M. Polito, F. Grepioni, *Struct. Bonding* **2004**, *111*, 1–32; c) D. Braga, *Chem. Commun.* **2003**, 2751–2754; d) D. Braga, M. Polito, M. Bracaccini, D. D'Addario, E. Tagliavini, L. Sturba, F. Grepioni, *Organometallics* **2003**, *22*, 2142–2150; e) D. Braga, L. Maini, M. Polito, L. Scaccianoce, G. Cojazzi, F. Grepioni, *Coord. Chem. Rev.* **2001**, *216–217*, 225–248; f) D. Braga, L. Maini, F. Paganelli, E. Tagliavini, S. Casolari, F. Grepioni, *J. Organomet. Chem.* **2001**, *637–639*, 609–615.

[18] A. Bondi, *J. Phys. Chem.* **1964**, *68*, 441–451.
[19] a) G. R. Desiraju, *Crystal Engineering: The Design of Organic Solid*, Elsevier, Amsterdam, **1989**, p. 129; b) G. Bhattacharjya, G. Savitha, G. Ramanathan, *CrystEngComm* **2004**, *6*, 233–235; c) X. Yang, D. Wu, J. D. Ranford, J. J. Vittal, *Cryst. Growth Des.* **2005**, *5*, 41–43.
[20] J.-L. Fillaut, J. Lineares, D. Astruc, *Angew. Chem.* **1994**, *106*, 2540–2542; *Angew. Chem. Int. Ed. Engl.* **1994**, *33*, 2460–2462.
[21] J.-L. Fillaut, D. Astruc, *J. Chem. Soc. Chem. Commun.* **1993**, 1320–1321.
[22] a) H. Puff, W. Schuh, R. Sievers, W. Wald, R. Zimmer, *J. Organomet. Chem.* **1984**, *260*, 271–280; b) J. Beckmann, M. Biesemans, K. Hassler, K. Jurkschat, J. C. Martins, M. Shürmann, R. Willem, *Inorg. Chem.* **1998**, *37*, 4891–4897.
[23] a) G. M. Sheldrick, SHELXL-97, Program for the Crystal Structure Refinement, University of Göttingen, Göttingen (Germany), **1997**; b) G. M. Sheldrick, SHELXTL, Reference Manual: Version 5.1, Bruker AXS, Madison (WI), **1998**.

Received: March 21, 2005
Published online: July 8, 2005